Integration of a microbial fuel cell into a green wall for greywater treatment

Gian Artur Bezzola

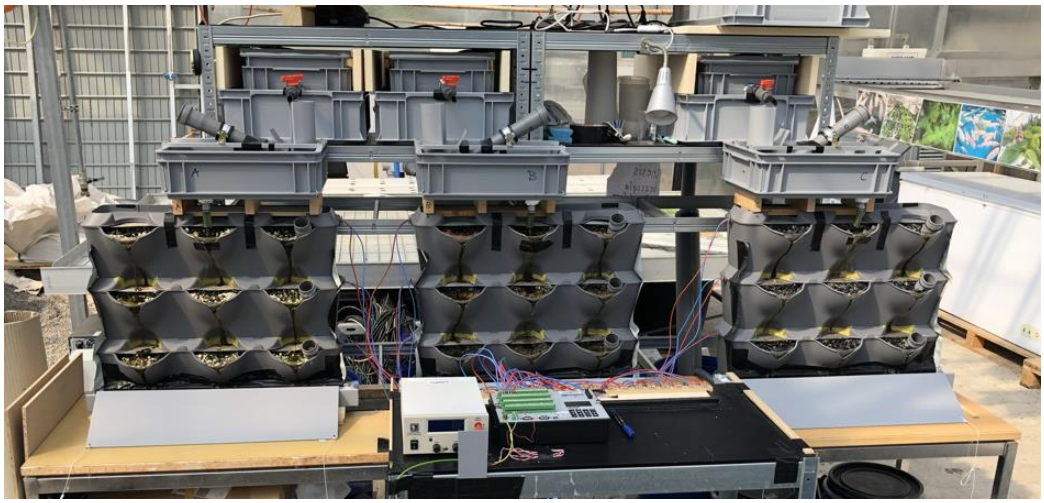

Supervisors:

Prof. Dr. Ranka Junge
ZHAW Life Sciences und Facility Management
Institut für Umwelt und Natürliche Ressourcen
Grüentalstrasse 14, 8820 Wädenswil

Nadine Antenen
ZHAW Life Sciences und Facility Management
Institut für Umwelt und Natürliche Ressourcen
Grüentalstrasse 14, 8820 Wädenswil

Imprint

Author:

Gian Artur Bezzola

E-Mail:

[redacted]

Keywords:

Microbial fuel cell, Electrochemical constructed wetland, Green wall, Synthetic greywater

Proposed citation:

Bezzola, G. A. (2022) Integration of a microbial fuel cell into a green wall for greywater treatment. Master Thesis. Wädenswil: Zürcher Hochschule für angewandte Wissenschaften (unpublished).

Name of the research institute:

Institut für Umwelt und natürliche Ressourcen (IUNR)

Zürcher Hochschule für angewandte Wissenschaften

Grüentalstrasse 14 Postfach

CH-8820 Wädenswil

Abstract

The aim of this master thesis was to investigate the influence of different reactor media on the electrical and cleaning performance of an electrochemical green wall (EGW). Another aim was to improve electrical power production and the treatment performance of the system investigated in Bezzola (2021). Therefore, the construction, inoculation and operation of the experimental installation based on the findings from Bezzola (2021). The reactor media studied were Vulkaponic (a plant substrate made of pumice and zeolite with a grain size of 3 - 7mm), Seramis (a fine-grained expanded clay), and HDPE biocarriers. The electrodes were constructed from biochar and stainless steel mesh. The system was inoculated over a time of 27 days with digested sludge from a wastewater treatment plant. Four measuring campaigns were conducted, at the beginning of which different quantities of greywater were added. The hydraulic retention time for each measuring campaign was 48 hours. The wall with Vulkaponic reactor medium generally resulted in the highest energy production values. This indicates that the substrate choice is a relevant parameter in EGW design. The electrode spacing is another relevant parameter in EGW design. The improved wall design resulted in increased treatment performance compared to the system investigated in Bezzola (2021). By increasing the hydraulic retention time, there is potential for a further improvement in treatment performance. The averaged maximum power per reactor was 5E-05 W/reactor. However, peak power density per reactor varied and could reach as much as 20E-05 W/reactor. Even for a large-scale green wall this power production is way too small to operate an electrical consumer. However, the power measurements could be used as an important indicator to characterize the state of the system in terms of bacterial activity. It could therefore be used in addition to the water quality parameters to optimally monitor, control and feed the system.

Table of contents

1 Introduction 6
2 Research questions and hypotheses 9
2.1 Research questions 9
2.2 Hypotheses 9
3 Material and methods 9
3.1 Green wall system 9
3.1.1 Assembling of the reactors 10
3.1.2 Reactor materials 10
3.1.3 Electronic design 10
3.2 Comparison of the performance with literature 11
3.2.1 The planting of the green walls 11
3.3 System design, hydraulic setup, and water flow through the system 11
3.4 Operation and monitoring 13
3.4.1 Greywater 13
3.4.2 Inoculation 14
3.4.3 Experiment 14
3.4.4 Performance of the EGW 17
3.4.5 Basic settings of the systems 18
4 Results 19
4.1 Water quality 19
4.2 Power generation 21
4.3 Correlations of power density and water quality indicators 25
5 Microbiology 27
5.1 Introduction 27
5.2 Materials and Methods 27
5.3 Results 28
6 Discussion 29
6.1 Possible usage of the generated power 29
6.2 Comparison of the performance with literature 29
7 Conclusion 33
8 Bibliography 34

Terms and Abbreviations

BOD	Biological oxygen demand
COD	Chemical oxygen demand
CW	Constructed wetland
DAS	Dewatered alum sludge
ECW	Electrochemical constructed wetland
EGW	Electrochemical green wall
GAC	Granular activated carbon
HLR	Hydraulic loading rate
HRT	Hydraulic retention time
LR	Loading rate
MFC	Microbial fuel cell
MO	Microorganisms
PEM	Proton exchange membrane
TN	Total Nitrogen
TP	Total Phosphorus
TOC	Total Organic Carbon
SSM	Stainless steel mesh

1 Introduction

Water scarcity is increasingly becoming a global problem. As of 2021, 2.3 billion people live in water stressed countries (UN-Water, 2021). Water stress meaning, that more than 25% of a country's renewable water resources are withdrawn (UN-Water, 2021). This applies above all, but not only, to developing countries (UN-Water, 2021). To mitigate water scarcity and stress, the U.N. general assembly promotes an increase of water-use efficiency across all sectors and to ensure sustainable withdrawals and supply of freshwater (U.N. General Assembly, 2017). One way to accomplish this is the discharge of treated household wastewater to recharge groundwater (Asano, 2016; Bouwer, 2002). This can have a profound impact, as 16% of all water withdrawals are used for households and services (UN-Water, 2021). However, even more important than using treated discharge to recharge the groundwater, is it to keep the used water out of the wastewater cycle for as long as possible. To achieve this, the water should be recycled at least once (Gross et al., 2015).

Household wastewater can be divided into heavily polluted blackwater containing urine, feces, flushing water, and dry matter for cleaning from the toilet (Gross et al., 2015) and lightly polluted greywater containing all other flows (e.g. kitchen, shower, washing machine, dishwasher) (Gross et al., 2015). In case of mixed sewer systems, stormwater is also included in the wastewater (Davis, 2010).

In the industrialized countries, the treatment of household wastewater is mostly carried out in centralized plants fed by an extensive sewer network (De Gisi et al., 2018; Heinss et al., 2004). Centralized wastewater treatments plants systems are most common in high-income countries (UNESCO World Water Assessment Programme, 2017).

While such systems are highly efficient and user friendly, they require large investments in infrastructure (treatment plant and sewer network), are characterized by high operation and maintenance costs, (Heinss et al., 2004) and demand large amounts of power (Rothausen and Conway, 2011). As a result, even when centralized wastewater treatment plants are built in developing countries, they fail in the long term. For example, in the 2000s, Malaysia had 91 centralized wastewater treatment plants. Of these, 89 had malfunctioned or failed (Laugesen et al., 2010). Also, many regions in developing countries would not be able to provide an adequate water supply to operate an extensive sewer system (Laugesen et al., 2010).

Therefore, it makes sense to construct and operate decentralized, near-natural, low-cost, low-energy, low-maintenance systems, that still have a high performance (Mara, 2004).

The use of decentralized systems can also be worthwhile in developed countries since this can improve the resilience and the efficiency of the treatment system (Novotny and Brown, 2007). Another important point is that the sewerage and technical systems of centralized systems have to be replaced after 50 to 100 years, which is associated with enormous costs. In most developed countries this is going to be the case in the near future (Laugesen et al., 2010).

Since greywater does not contain blackwater, its organic load and microbial contamination are lower. This enables it to be treated on-site with relatively simple systems (Gross et al., 2015).

Constructed wetlands (CWs) can be a suitable treatment system in this case because they are relatively inexpensive. They have low operation and maintenance requirements, a high treatment effectiveness, and their performance is less sensitive to input variations (Dotro et al., 2017; Gross et al., 2015). CWs can treat many different types of wastewater. CWs

usually consist of a gravel or sand bed and are planted with emergent macrophytes (Dotro et al., 2017). The wastewater flow through a CW is either vertical or horizontal (Dotro et al., 2017). The planting with emerging macrophytes provides additional benefits (e.g. stabilization of the CW bed surface stabilization, root release of oxygen) (Brix, 1994).

CWs treat wastewater through physical processes (e.g. sedimentation and filtration of suspended solids, particulate organic matter, and pathogens), chemical processes (e.g. precipitation of phosphorous compounds), and biological processes (e.g. plant uptake of phosphor and nitrogen, microbiological (de)nitrification) (Dotro et al., 2017). When factors like the space requirement for sewers for centralized treatment plants are considered, CWs can use less land than centralized wastewater treatment plants (Fan et al., 2021).

Constructed wetlands also have the potential to be designed as microbial fuel cells (MFCs) for the additional production of energy. MFCs convert the chemical energy in organic matter into electrical energy. This conversion is made by anaerobic, exoelectrogenic bacteria. A MFC consists of two half cells, the anode and cathode chambers, containing the electrodes. Both chambers are filled with liquid medium. The electrodes are connected via an external circuit, to which an electrical consumer can be connected (Logan, 2008).

The exoelectrogenic bacteria grow on the anode, therefore anaerobic conditions must be prevalent in the anode chamber. To maintain these, the mixing of the liquids in the anode and cathode chambers has to be avoided. The separation of both has to be done with a proton exchange membrane (PEM), so that the protons created at the anode can travel to the cathode (Logan, 2008).

The bacteria are fed with organic matter, which they oxidize into electrons and protons. The electrons are released to the anode and travel through the external circuit and the consumer to the cathode. The protons are released into the liquid medium and pass through the PEM into the cathode chamber. At the cathode, the protons are reduced to water using oxygen as the reducing agent, thus completing the chemical reaction (Logan, 2008).

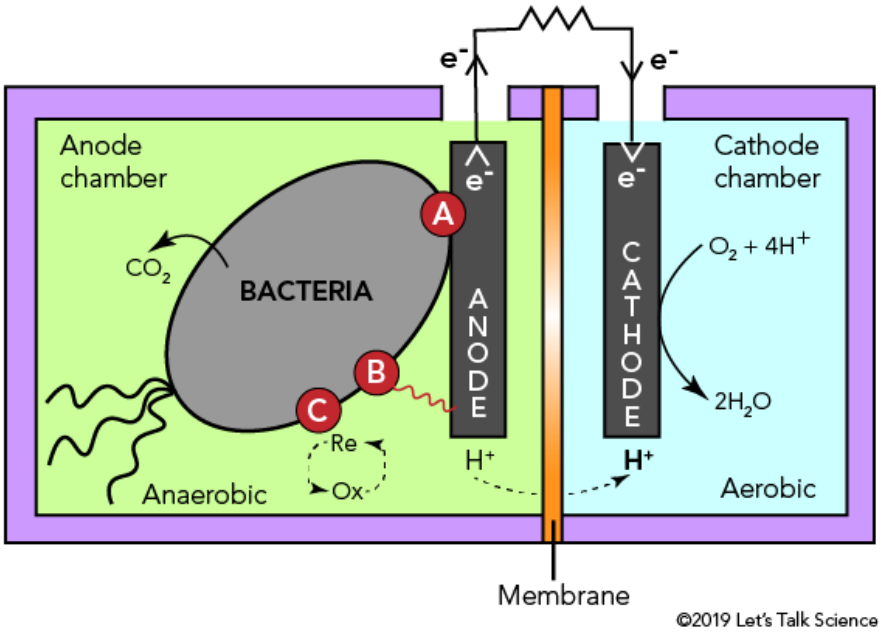

Figure 1: Schematic representation of the structure and function of an MFC (Pop, 2019)

An MFC can be integrated into CW to create an electrochemical constructed wetland (ECW). This is possible because the wastewater introduces a constant flow of organic matter into a CW (Dotro et al., 2017). In an ECW the PEM can be omitted, because the oxygen (redox) gradient naturally occurring in CWs between the aerobic upper zone at the water surface and the anaerobic lower zone at the bottom of the treatment bed fulfills the same function (Corbella et al., 2014).

To save space and allow an indoor usage, multiple ECWs can be stacked to form an electrochemical green wall (EGW) (Osorio de la Rosa et al., 2019). The feasibility of such a system has already been proven (Bezzola, 2021).

The results obtained by Bezzola (2021) were in a comparable range to the results found in the literature in terms of hydraulic retention time (HRT) and the removal rate of the chemical oxygen demand (COD) (Table 1). However, the average power density observed in Bezzola (2021) was about 20 times lower than the average values from the literature review. However, this value is still within the range of the power densities from the literature review. These relatively low power densities can operate only the smallest electrical consumers, but it should be possible to increase these power densities with an improved system.

Table 1: Comparison of the average values (range in brackets) for HRT, COD removal rate, and power density found in the literature for comparable systems (Comparison of the performance with literature (without this study) and Bezzola (2021)

Parameters	MFC & CW (Literature review)	MFC & GW (Bezzola, 2021)
HRT [h]	75 (24 – 144)	120
COD removal rate [%]	82 (56 – 100)	86
Power density [W/l]	6.6E-05 (6.02E-07 – 3.21E-04)	3.1E-06

2 Research questions and hypotheses

The following research questions and hypotheses were formulated for this master's thesis:

2.1 Research questions

- How is it possible to increase the generation of electrical power of an EGW?
- Do the choice of the substrate and the wastewater load influence the power generation and the treatment performance of an EGW?

2.2 Hypotheses

- The selection of suitable substrates can increase the treatment performance and generated power of an EGW.
- A change in the wastewater load into the system influences the generation of electrical power and the treatment performance.

3 Material and methods

3.1 Green wall system

Three green walls (A, B, and C) were constructed with the NatureUp! (Gardena, Ulm, Germany) green wall system. Each green wall consisted of three planters stacked on top of each other according to the manual (Figure 2) and covered an area of 0.363 m^2.

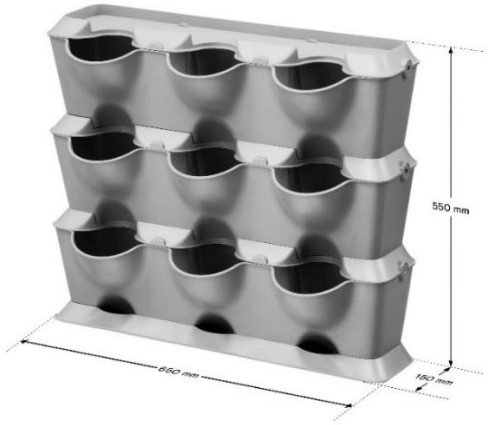

Figure 2: NatureUp! Green wall as used in the project consisting of three boxes assembled according to the manual.

Because it was not possible to combine the three planters of a green wall into a single EGW, a MFC was integrated into every single planter. Each planter was therefore designed as a reactor. The water cascaded from one reactor of the green wall to the next (Figure 5). To enable that, the drainage slits in every reactor were plugged using mounting adhesive.

To prevent flooding or wetting of the cathode, the water level in the reactors was lowered. To accomplish that, the three planting bulges of each reactor were incised with triangular notches with a depth of 30 mm and a width of 58 mm. These notches had the additional benefit of improving the water flow from each reactor.

3.1.1 Assembling of the reactors

All reactors were constructed according to Figure 3. The layers within the reactor consisted of an anode, made of biochar and stainless steel mesh (SSM) at the at the bottom, a substrate layer in the middle, and a cathode (also made of biochar and SSM) at the top. The thickness of the carbon layers and the position of the SSM of the anode were dictated by the geometry of the planter. The substrate layer in the center served as a spacer between the electrodes and as habitat for the microorganisms.

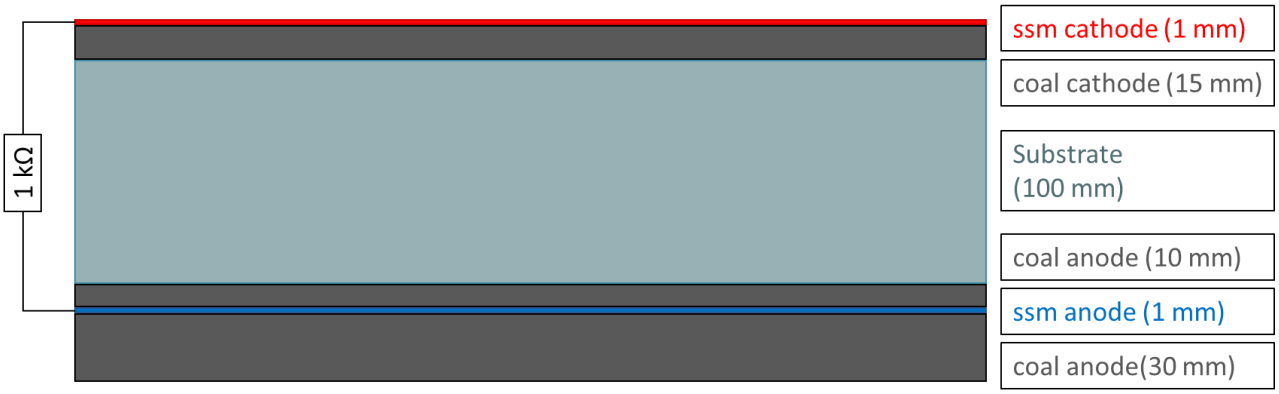

Figure 3: Schematic diagram of the layered structure and the external electrical circuit of a single reactor.

In order to insert the probes to monitor the abiotic parameters in the anaerobic zone of the reactors, a polypropylene drainpipe with a diameter of 40 mm was installed in each reactor and extended down to the SSM of the anode (Figure 18).

3.1.2 Reactor materials

Three substrates were tested as reactor media (Table 2). The mineral plant substrate Vulkaponic was used because the pre-trial results in Bezzola (2021) were promising. As a second mineral plant substrate, expanded clay (Seramis) was used. To compare them to an inorganic substrate, biocarriers (Table 2) were tested.

Table 2: Description and properties of the reactor materials used.

EGW	Material	Company	Description	Bulk density [g/l]	Porous water capacity [%]
A	Vulkaponic 3/8	Klanz, Altenholz, Germany	Mineral substrate of pumice and zeolite for indoor plants	659	42.0
B	Seramis	Westland, Mogendorf, Germany	Expanded clay substrate for indoor plants	677	43.0
C	Biocarriers		HDPE biocarriers, 10x10 mm, surface area of approx. 800m^2 per m^3	166	81.5
All electrodes	Biochar	Verora AG, Edlibach, Switzerland	Pyrolyzed vegetable charcoal	490	47.0

3.1.3 Electronic design

The SSMs of the anode and cathode were connected via an external circuit. An electrical resistor with a resistance of 1000 ohms was used as an electrical load in the external circuits, because it was the most used resistance by other studies (see Discussion

Possible usage of the generated power

The averaged maximum power per reactor was 5E-05 W/reactor. The peak maximum power density per reactor was four times higher at 20E-05 W/reactor. A Wall in this study covers an area of 0.363 m2. The indoor green wall in the train station in Shin-Yamaguchi in Japan covers a surface of 400 m2 (Blanc, 2013). It would be possible to fit approx. 1100 subunits, with an averaged maximum power of 5E-05 W per subunit or a peak maximum power density of 20E-05 W, on this area. This would result in a total power of 0.055 W and 0.22 W respectively. This is an extremely small power, which in reality could hardly operate an electrical consumer. For comparison, a modern LED light bulb requires about 6-9 W of power.

3.2 Comparison of the performance with literature

Table 16). All circuits were connected to a datalogger, which measured the voltages of the reactors in every second. The average of the measurements was calculated and written in by the logger in 10 second intervals. The voltages were also measured independently in longer time intervals with a multimeter at the screw terminals of the datalogger (Figure 4.). Only the latter were used for the analysis. The measurements of the data logger were only used as comparison values.

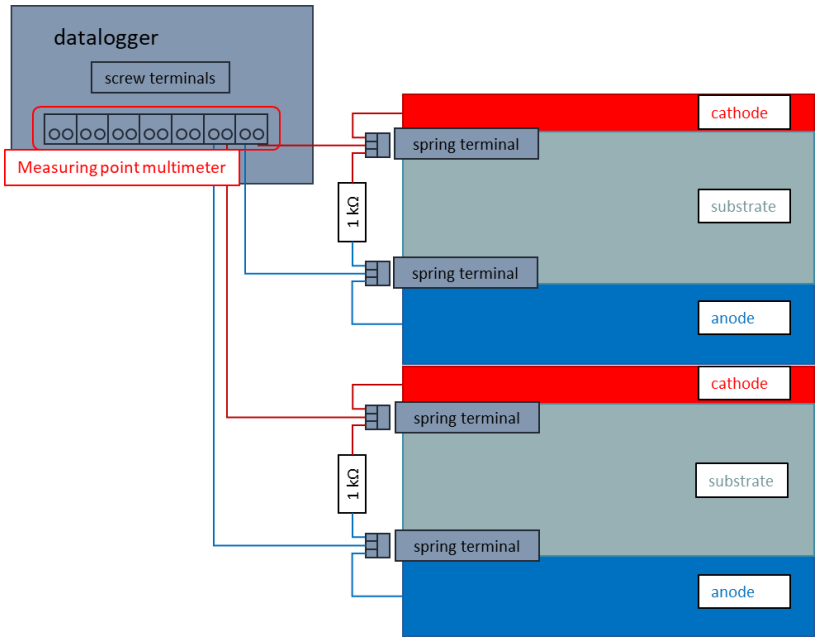

Figure 4: Schematic of the electronic design.

3.2.1 The planting of the green walls

In order for the plants to exert an impact on the performance of the system, they would have needed enough time to spread the roots through the substrate. Also, roots exude oxygen and carbon-based compounds. In order to avoid this, the walls were not planted.

3.3 System design, hydraulic setup, and water flow through the system

Each green wall had its own water circuit. It consisted of a reservoir from which the water was pumped upwards into an elevated tank. This tank continuously overflowed into a collection container. Thus, the pressure in the elevated tank permanently remained the same. From the elevated tank the water was fed into the green wall. The regulation of the water flow was done by a valve. The water cascaded from one reactor of the green wall to

the next (Figure 5). After cascading through the green wall, the water was fed back into the reservoir. The water captured in the collection container was directly fed back into the reservoir. To prevent the water from just cascading through the reactors without mixing, the flow rate was limited to between 0.0021 and 0.0022 liters per second.

During the inoculation the reactors were continuously fed with water from the reservoir. For the experiment, the water feeding mode of the reactors was changed to a periodic surge feed. This was done through a mechanical dosing apparatus modeled after a Japanese Shishi-odoshi (Figure 19) (Miyazaki and Yamada, 2016). The apparatus had a volume of 0.3 liters and emptied in an interval of 39 seconds.

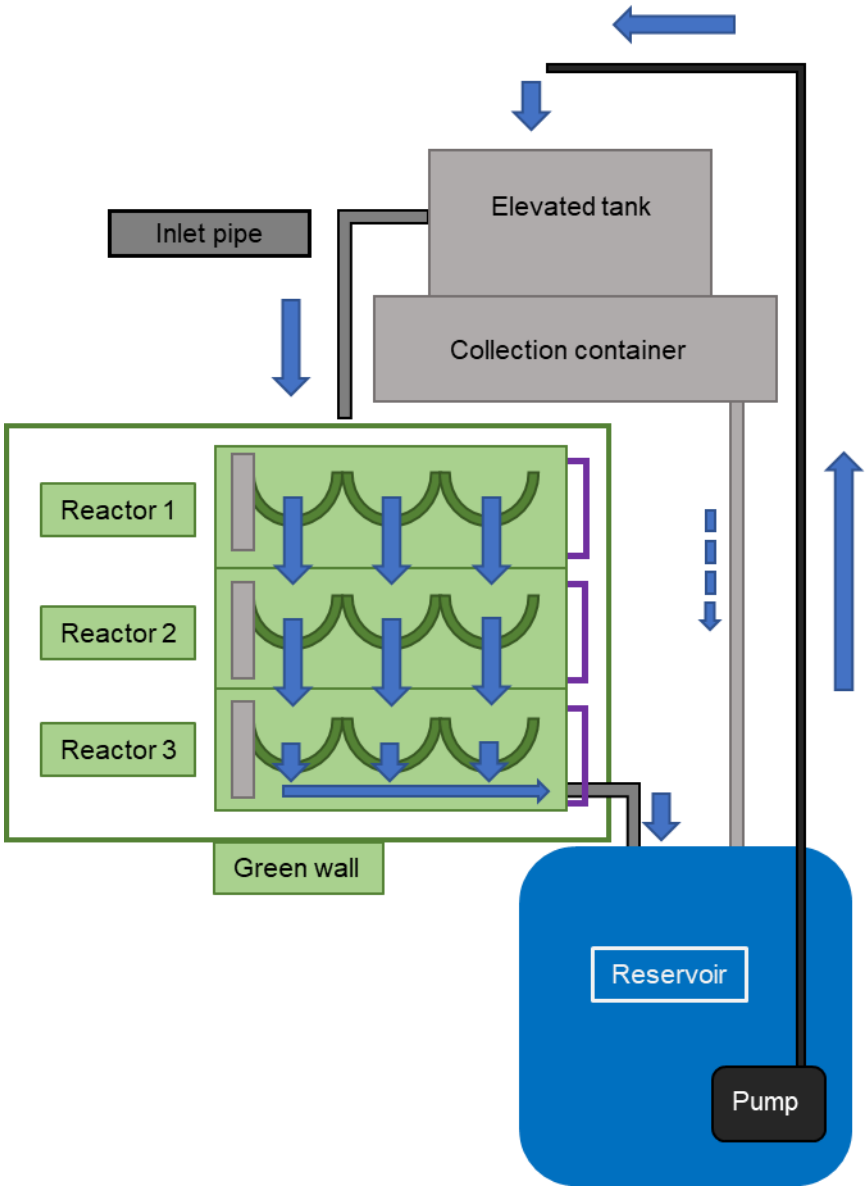

Figure 5: Schematic diagram of a complete single green wall system including the water flow.

3.4 Operation and monitoring

After the construction of the system was finished, the reactors of the green walls were inoculated for 27 days. Three measuring campaigns were conducted in calendar weeks 48, 49, 50 of the year 2021. A fourth measuring campaign was conducted in the first week of 2022.

3.4.1 Greywater

For a consistent and comparable performance between the three systems, a synthetic greywater was used. The greywater recipe (Table 3) was based on Hourlier et al. (2010), Pradhan et al. (2019), and Prodanovic et al. (2019) and was also used in a previous study (Bezzola, 2021).

Table 3: Recipe of the synthetic greywater to be used in this thesis

Ingredient	Brand	Product	Place of purchase	Concentration in greywater (mg/l)
Shampoo	Schwarzkopf	schauma - fresh it up shampoo	Lidl	20
Moisturizer	Cien	Classic moisturising cream (Grapeseed oil & shea butter)	Lidl	10
Toothpaste	Nevadent	Complex 7 total care plus	Lidl	10
Deodorant	Nivea	Fresh pure 0% Aluminium	Lidl	10
Handwash	Cien	Handwash Almond	Lidl	30
Liquid laundry detergent	Ariel	Color +	Lidl	250
Fabric softener	Comfort	Concentrate pure	Lidl	210
Dishwashing detergent	Pril	Kraftgel Ultra Plus	Lidl	300
Vinegar	Migros	Apfelessig	Migros	250
Vegetable oil	Mbudget	Pflanzenöl	Migros	250
Corn starch	Pâtissier	Maisstärke	Migros	150
Cellulose	-	Cellulose microcrystalline for column chromatography	Merck	100
Urea	-	-	-	10
Lactic acid	-	-	-	40
Soil	-	-	-	100
KH_2PO_4	-	-	-	3.5

For the inoculations and the experiment, the synthetic greywater was prepared as a stock solution in the required quantity to achieve the desired concentration in each reactor. This stock solution was subsequently mixed with the 60 liters of tap water which represents the total volume of fluid in each green wall system.

3.4.2 Inoculation

To facilitate the growth of the required exoelectrogenic bacteria, the green walls were inoculated with digested sludge from the wastewater treatment plant Wädenswil-Rietliau, Switzerland. The unfiltered and undiluted sludge was injected directly into the anaerobic zone of the reactors with a large syringe. Additional digested sludge was introduced into the hydraulic circuit via the reservoirs (Table 4). The amount of digested sludge added to the reactors was based on experience values obtained from Bezzola (2021).

Table 4: Amount of digested sludge that was used in the inoculations.

	Amount of digested sludge injected per green wall [ml]	Amount of digested sludge mixed in per reservoir [ml]
First inoculation (week 44)	360	720
Second inoculation (week 45)	360	360
Third inoculation (week 46)	540	0

To feed the microorganisms (MOs), synthetic greywater was also added (Table 5). During the inoculation the greywater concentration was gradually increased to allow the adaptation of the MO to the greywater concentrations used in the experiment.

Table 5: Greywater concentrations used during the inoculations of the reactors

Ingredient	Concentration 1st inoculation [g/l]	Concentration 2nd inoculation [g/l]	Concentration 3rd inoculation [g/l]
Shampoo	0.010	0.015	0.020
Moisturizer	0.005	0.008	0.010
Toothpaste	0.005	0.008	0.010
Deodorant	0.005	0.008	0.010
Handwash	0.015	0.023	0.030
Liquid laundry detergent	0.125	0.188	0.250
Fabric softener	0.105	0.158	0.210
Dishwashing detergent	0.150	0.225	0.300
Vinegar	0.125	0.188	0.250
Vegetable oil	0.125	0.188	0.250
Corn starch	0.075	0.113	0.150
Cellulose	0.050	0.075	0.100
Urea	0.005	0.008	0.010
Lactic acid	0.020	0.030	0.040
Soil	0.050	0.075	0.100
KH2PO4	0.00175	0.002625	0.00350

3.4.3 Experiment

Four measuring campaigns were conducted during the experiment. Prior to each measuring campaign, the elevated tank, collection container and reservoir of each system were emptied and cleaned in preparation. The pumps were also cleaned. Each system was then filled up with fresh water to the starting volume of 60 l.

Each measuring campaign spanned three days. Because the water samples were taken in the morning on each day of measuring campaigns, this corresponds to an HRT of about 48 hours, that the water spent in each system.

On the first day of each measuring campaign, the pumps were turned off in all three systems. After a short wait to ensure that all the water in the system (except for the residual water in the walls) had collected in the reservoir, the greywater stock solution in the required concentration was then poured into each reservoir in the desired quantity (Table 7) and then subsequently stirred. The pumps were then switched on again. After waiting for about 10 minutes, the water samples for the laboratory analysis (Table 8) were taken. The taking, treatment and analysis of the water samples was done according to Table 6.

After measuring campaign 4, the systems continued to operate for two months. In the first month, the systems were fed a total of three times with the same amount of greywater as in measuring campaign 4. In the second month, the system was fed two times more with half the amount of greywater each time. During the entire time, evaporation losses were compensated by the addition of tap water, so that a constant amount of liquid was present in the systems over the entire time. The evolution of power density over the entire duration of the operation is shown in Figure 6.

Table 6: Schedule of each measuring campaign

Day 1	Day 2	Day 3
Drawing Water samples	Drawing Water samples	Drawing Water samples
Measure voltage via multimeter	Measure voltage via multimeter	Measure voltage via multimeter
Measure abiotic parameters	Measure abiotic parameters	Measure abiotic parameters
Readout measured voltages of the datalogger	Readout measured voltages of the datalogger	Readout measured voltages of the datalogger
Preparation biological oxygen demand over 5 days (BOD_5) analysis	Preparation BOD_5 analysis	Preparation BOD_5 analysis

Table 7: Greywater concentrations for the measuring campaigns

Ingredient	Greywater concentrations measuring campaigns 1, 2, and 3 [g/l]	Greywater concentration measuring campaign 4 [g/l]
Shampoo	0.020	0.010
Moisturizer	0.010	0.005
Toothpaste	0.010	0.005
Deodorant	0.010	0.005
Handwash	0.030	0.015
Liquid laundry detergent	0.250	0.125
Fabric softener	0.210	0.105
Dishwashing detergent	0.300	0.150
Vinegar	0.250	0.125
Vegetable oil	0.250	0.125
Corn starch	0.150	0.075
Cellulose	0.100	0.050
Urea	0.010	0.005
Lactic acid	0.040	0.020
Soil	0.100	0.050
KH2PO4	0.00350	0.00175

Table 8: Water sampling and analysis

Parameter	Place of sampling	Measurement interval	Sample size and container per wall	Sample preparation	Sample storage	Measurement equipment	Company
Total nitrogen (TN), Total organic carbon (TOC)	SP Inlet pipe of the green wall	Every day of a measuring campaign	2 X 40 ml in a 50 ml centrifuge tube	-	Put in freezer	TOC-L Analyzer and ASI-L	Shimadzu Europa GmbH, Duisburg, Germany
Total phosphorus (TP)	SP Inlet pipe of the green wall	Every day of a measuring campaign	50 ml centrifuge tube with COD	-	Put in freezer	LCK349 Phosphorus total / phosphate ortho cuvette test	Hach Lange, Düsseldorf, Germany
Ammonium (NH_4^+),	SP Inlet pipe of the green wall	Every day of a measuring campaign	10 ml in a 15 ml centrifuge tube	Syringe filtration (0.45 µm) + acidification with approx. 0.5 ml HNO_3	Put in freezer	930 Compact IC Flex	Metrohm Schweiz AG, Zofingen, Schweiz
Nitrite (NO_2^-), Nitrate (NO_3^-), Phosphate (PO_4^-)	SP Inlet pipe of the green wall	Every day of a measuring campaign	10 ml in a 15 ml centrifuge tube	Syringe filtration (0.45 µm)	Put in freezer	930 Compact IC Flex	Metrohm Schweiz AG, Zofingen, Schweiz
COD [mg/l]	SP Inlet pipe of the green wall	Every day of a measuring campaign	50 ml centrifuge tube with PO_4^-	-	Put in freezer	LCI400 COD cuvette test	Hach Lange, Düsseldorf, Germany
BOD_5 [mg/l]	SP Reservoir of the green wall	Every day of a measuring campaign	500 ml sample bottle	-	Analyzed right away	OxiTop	Xylem Inc., Rye Brook, USA

3.4.4 Performance of the EGW

To assess the performance of the EGW the values in Table 9 were calculated from the analyzed water samples (Table 8). Table 10 gives an overview of the basic measured parameters.

Table 9: Values calculated from the basic measured parameters

Parameters	Definitions	Used variables
Flow rate (Q) [l*s^{-1}]	$Q = V/t$	V: Measured volume [l] t: Measured time [s]
HRT [h]	$HRT = V/Q/3600$	V_R: Reactor volume [l] Q: Flow rate through the reactor [l/s]
Hydraulic loading rate (HLR) [l*m^{-2}*d^{-1}]	$HLR = Q/A/(3600 * 24)$	Q: Flow rate through the reactor [l/s] A: Infiltration area of the system [m2]
Power [W]	$P = (U^2/1000)/R$	U: Measured voltage [mV] R: External resistance [kΩ]
Power density [W *l^{-1}]	$PD_V = \mathrm{P}/V$	U: Calculated power [W] V: Reactor volume [l]
Loading rates (LR) for TOC, COD, BOD5, TN, TP [mg*m^{-2}*s^{-1}]	$OLR_{BOD5} = Q * \beta_{Substance}/A$	Q: Flow rate through the reactor [l/s] $\beta_{Substance}$: Substance-concentration A: Infiltration area of the system [m2]
Removal-rates for TOC, COD, BOD5, TN, NH_4^+, NO_2^-, NO_3^-, TP, and PO_3^{4-} [%]	$Rr = 100 - Conc_{init}/Conc_{fin}$	$Conc_{fin}$: Final concentration [mg/l] $Conc_{init}$: Initial concentration [mg/l]
Oxygen-saturation [%]	$O_{2Sat} = DO_{conc.} * 100/O_{conc.\ atmos}$	$DO_{conc.}$: Concentration of dissolved oxygen in water [mg/l] $O_{conc.\ atmos}$: Equilibrium oxygen concentration in the atmosphere at 10°C and an elevation of 515 m [mg/l]

Table 10: Basic measured parameters

Parameter	Place of measurement	Measurement interval	Measurement equipment	Company
Reactor volume [l]	-	Once	Measuring vessel	-
Infiltration area of the system [m^2]	-	Once	Folding rule	-
Time [s]	-	Every day of a meas. campaign	Stopwatch	-
Volume of recirculating fluid [l]	SP Inlet pipe of the green wall	Every day of a meas. campaign	Measuring vessel	-
Voltage [mV]	SP external electrical circuits 1, 2 and 3	2-4 times every day of the experiment	PROFI DEPOT Digital-Multimeter MM 7700	BAUHAUS Fachcentren AG, Belp, Switzerland
Dissolved oxygen (DO) [mg/l]	SP Measurement tubes 1, 2 and 3 in the reactors	Every day of a meas. campaign	Multimeter HQ40D Probe LDO101	Hach Lange, Düsseldorf, Germany
Oxygen redox potential (ORP) [mV]	SP Measurement tubes 1, 2 and 3 in the reactors	Every day of a meas. campaign	Multimeter HQ40D Probe LDO101	Hach Lange, Düsseldorf, Germany
pH	SP Measurement tubes 1, 2 and 3 in the reactors	Every day of a meas. campaign	Multimeter HQ40D Probe PHC101	Hach Lange, Düsseldorf, Germany
Temperature [°C]	SP Measurement tubes 1, 2 and 3 in the reactors	Every day of a meas. campaign	Multimeter HQ40D Probe PHC101	Hach Lange, Düsseldorf, Germany
Electrical conductivity (EC)	SP Measurement tubes 1, 2 and 3 in the reactors	Every day of an experiment	Multimeter HQ40D Probe CDC401	Hach Lange, Düsseldorf, Germany
Turbidity [FNU]	SP Reservoir of the green wall	Every day of a meas. campaign	Turbidimeter 2100Q IS	Hach Lange, Düsseldorf, Germany

3.4.5 Basic settings of the systems

The basic settings of the three walls are listed in Table 11.

Table 11: Technical Specifications for the system

Parameter	Wall A: Vulkaponic (pumice and zeolite)	Wall B: Seramis (expanded clay)	Wall C: HDPE biocarriers
Flow rate [l*s^{-1}]	0.0021	0.0022	0.0022
Liquid volume per reactor [l]	3.8	3.9	6.3
HRT in a system [h]	48	48	48
HRT in a reactor [h]	0.61	0.60	0.99
Average HLR [l*m-2*d-1]	1981	2046	2055
Average TOC LR [mg*m^{-2}*s^{-1}]	3.46	3.32	3.48
Average COD LR [mg*m^{-2}*s^{-1}]	11.6	11.7	12.1
Average BOD_5 LR [mg*m^{-2}*s^{-1}]	8.5	8.7	9.0
Average TN LR [mg*m^{-2}*s^{-1}]	0.13	0.12	0.19
Average TP LR [mg*m^{-2}*s^{-1}]	0.07	0.07	0.12

4 Results

4.1 Water quality

The averages of water quality indicators (Table 12) were assessed for each reactor. Subsequently, the mean values and standard deviations averaged over the experiment were calculated for each system.

Table 12: Average (mean ± SD) values of various measured or calculated water quality parameters measured or calculated from the data of the EGWs A (Vulkaponic substrate), B (Seramis expanded clay), and C (HDPE biocarriers)

	System A			System B			System C			
Parameter	**Start conc.**	**End conc.**	**Removal rate [%]**	**Start conc.**	**End conc.**	**Removal rate [%]**	**Start conc.**	**End conc.**	**Removal rate [%]**	**n**
BOD_5 [mg/l]	654.1 ± 228.7	125.3 ± 19.7	80 ± 4	696.4 ± 208.5	127.3 ± 21.1	81 ± 3	745.9 ± 238.9	111.3 ± 2.0	84 ± 5	6
COD [mg/l]	835.5 ± 309.0	307.3 ± 79.7	60 ± 14	831.8 ± 244.3	289.5 ± 49.1	63 ± 10	905.0 ± 335.0	266.3 ± 54.8	68 ± 12	12
TOC [mg/l]	9.0 ± 2.1	5.4 ± 2.5	60 ± 8	8.4 ± 2.2	4.8 ± 2.5	63 ± 9	10.7 ± 2.2	7.2 ± 3.0	48 ± 15	12
TN [mg/l]	236.4 ± 60.11	147.7 ± 70.45	57 ± 9	221.2 ± 55.8	143.1 ± 58.1	58 ± 8	244.6 ± 53.4	137.7 ± 74.2	62 ± 11	12
Ammonium [mg/l]	0.006 ± 0.1	0.0 ± 0.0	25 ± 50	0.3 ± 0.5	0.0 ± 0.0	25 ± 50	0.0 ± 0.0	0.5 ± 1.0	0 ± 0	12
Nitrite [mg/l]	3.0 ± 0.5	1.9 ± 1.3	34 ± 49	3.2 ± 1.1	1.7 ± 1.1	36 ± 46	3.5 ± 0.5	0.7 ± 1.3	82 ± 34	12
Nitrate [mg/l]	4.4 ± 2.9	2.5 ± 0.5	23 ± 49	5.8 ± 3.2	2.3 ± 0.3	44 ± 44	4.5 ± 4.2	4.0 ± 2.1	-52 ± 119	12
TP [mg/l]	4.7 ± 0.9	2.2 ± 0.2	52 ± 9	4.6 ± 1.1	1.7 ± 0.3	62 ± 7	6.3 ± 1.3	4.3 ± 0.6	32 ± 7	12
Phosphate [mg/l]	7.1 ± 0.8	3.7 ± 0.2	48 ± 7	7.6 ± 1.5	3.6 ± 0.1	51 ± 9	8.4 ± 0.8	4.7 ± 1.2	44 ± 15	12
DO [mg/l]	0.3 ± 0.4			0.3 ± 0.2			0.2 ± 0.2			13
O_2-saturation [%]	2.8 ± 3.8			2.8 ± 1.9			1.9 ± 1.9			13
EC [µS/cm]	498.9 ± 38.0			558.8 ± 90.8			534.8 ± 38.0			12
ORP [mV]	-292.1 ± 38.7			-259.4 ± 60.9			-279.1 ± 51.2			10
Turbidity [FNU]	62.2 ± 13.0			75.9 ± 16.4			71.5 ± 24.5			14
pH	7.5 ± 0.2			7.4 ± 0.2			7.4 ± 0.2			13

The BOD_5 removal rates in systems A,B, and C (80 ± 4%, 81 ± 3%, and 84 ± 5% respectively) were very similar to each other.

The COD removal rates in systems A, B, and C (60 ± 14%, 63 ± 10%, and 68 ± 12% respectively) were also similar to each other. However, they were about 20 – 25% smaller than the BOD5 removal rates and fluctuated a bit more than the COD removal rates.

The TOC removal rates in systems A and B (60 ± 8% and 63 ± 9%) were similar to each other and to the COD removal rates of systems A and B. The TOC removal rate in system C was lower at 48 ± 15%.

The TN removal was comparable in systems A, B, and C (57 ± 9%, 58 ± 8%, and 62 ± 11% respectively). Nevertheless, since there was a clear degradation of TN in all three systems, it can be concluded that denitrification also occurred in the systems. The high relative abundance of bacteria of the genus Pseudomonas in Bezzola (2021) (Figure 9), which may include denitrifying species (Timmons and Ebeling, 2010), is another indication that denitrification may have occurred in the reactors.

In all three systems, the concentrations of ammonium were close to zero at all times, which might be due to nitrification. The already low initial concentrations may indicate that this could have already occurred during mixing or storage of the greywater concentrate.

The nitrite removal rates in systems A and B (34 ± 49% and 36 ± 46%) were similar, while the removal rate system C was higher with 82 ± 34%. However, all the removal rates fluctuate strongly and thus can hardly be compared. The nitrite concentrations, which are also very low, are another indication that nitrification occurred.

The nitrate removal rates in the systems A, B, and C (23 ± 49, 44 ± 44, and -52 ± 119 respectively) fluctuated wildly and were not comparable.

The TP removal rate of the systems A and B (52 ± 9% and 62 ± 7%) were comparable, while the removal rate of system C was much lower with 32 ± 7%.

The phosphate removal rates of the systems A, B ,and C (48 ± 7%, 51 ± 9%, and 44 ± 15% respectively) were closer to each other than the TP removal rates.

The mean dissolved oxygen concentration in the lower zone of all reactors was less than 0.3 mg/l. Moreover, the highest average oxygen saturation in the reactors was 2.8%. The lower zone of all reactors can therefore be considered anaerobic.

The EC values for the systems A, B, and C (498.9 ± 38.0 µS/cm, 558.8 ± 90.8 µS/cm, and 534.8 ± 38.0 µS/cm, respectively) were in a comparable range.

The ORP values of the systems A, B, and C (-292.1 ± 38.7 mV,-259.4 ± 60.9 mV, and -279.1 ± 51.2 mv respectively) were quite similar to each other.

The turbidity values of the systems A, B, and C (62.2 ± 13.0 FNU, 75.9 ± 16.4 FNU, and 71.5 ± 24.5 FNU respectively) were very similar to each other.

The pH was extremely similar in systems A, B, and C (7.5 ± 0.2, 7.4 ± 0.2, 7.4 ± 0.2, respectively) and remained practically constant over time.

4.2 Power generation

In order to be able to compare the results of the experiment with other studies , the power densities for walls A, B and C were calculated. To show that the power in most reactors changed considerably over time, the calculated power densities for each reactor over the entire duration from the first to the last measuring campaign and over the following two months are represented in Figure 6.

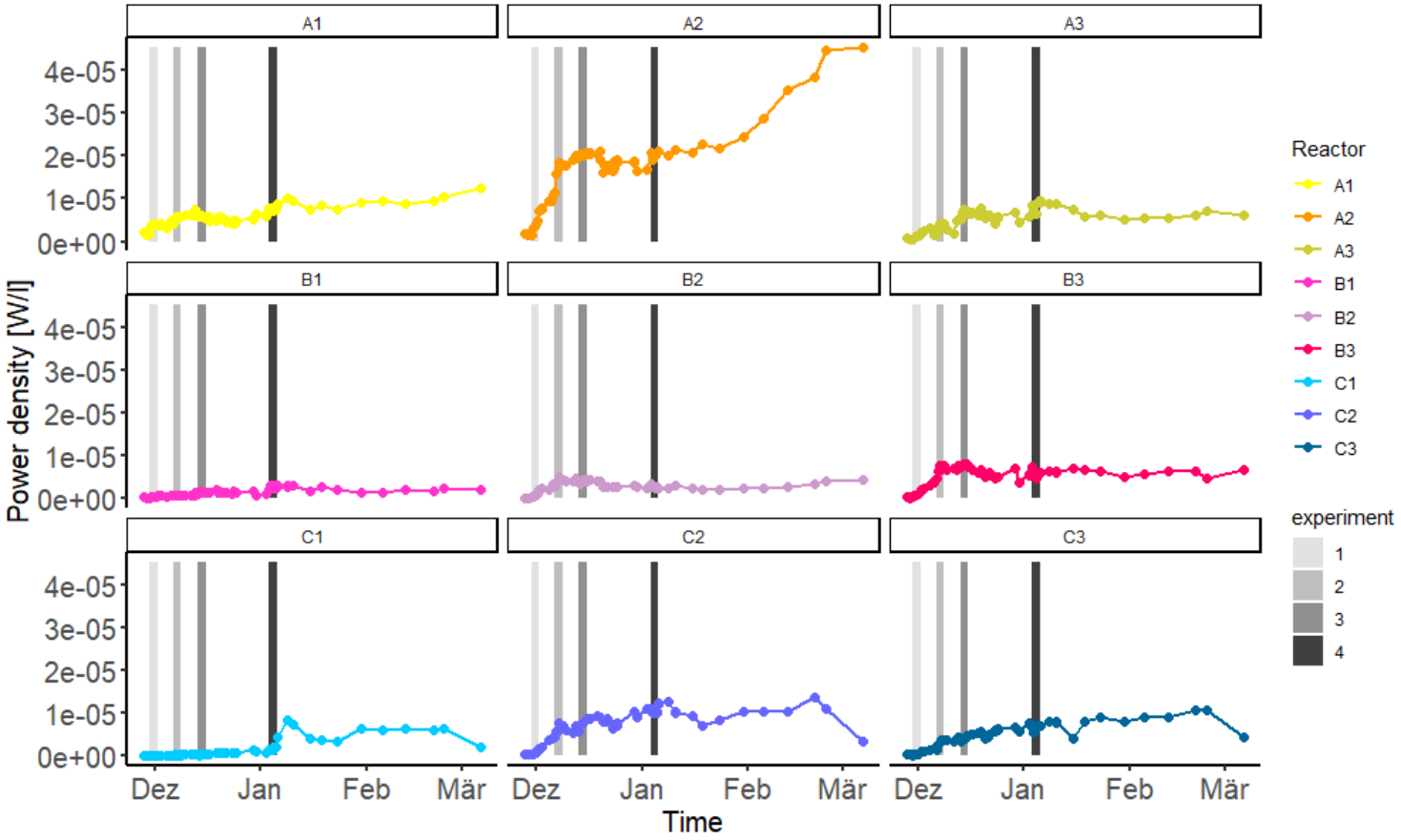

Figure 6: The electrical power densities generated by the EGW-systems A (Vulkaponic substrate), B (Seramis expanded clay), and C (HDPE biocarriers) as measured by multimeter and sorted by reactor, over the entire operation period of the system (starting with measuring campaign 1 and ending two months after measuring campaign 4). Three measuring campaigns were conducted in calendar weeks 48, 49, 50 of the year 2021. A fourth measuring campaign was conducted in the first week of 2022.

Figure 6 shows relatively clearly that the walls were evolving and that the measurements taken represented the state of the systems at different stages of development.

It has to be taken in consideration that constructed wetlands, for example, take months or even years to establish. Figure 6 suggests that this is also true for green walls. Thus, the measurements made represent four measurement campaigns in developing walls.

It appears that wall A (Vulkaponic) reached a certain energy production level more rapidly than the other two walls. In particular, in reactor A2 the development was relatively dynamic. It is characterized by two distinctive increases in production at the beginning and towards the end of the observed period. In contrast, walls B and C show a more continuous evolution of the energy production, which decreased towards the end of the period (decreasing graywater feed). For wall C (HDPE biocarriers), energy production developed much more slowly than for walls A (Vulkaponic) and B (Seramis expanded clay). The reason for this is probably that the biocarriers of wall C do not contain any mineral components and thus bacterial growth took significantly more time.

The largest increase in power density occurred in measuring campaigns 1 to 3, which were carried out with the larger wastewater load (Table 7), this increase can probably be attributed to the fact that the population of exoelectrogenic bacteria was not yet fully established after inoculation (Reactors A1 and B1 in Figure 6). However, it is difficult to draw conclusions about the influence of the wastewater load, since only measuring campaign 4 was carried out with the reduced wastewater load (Table 7).

At the last measurement point of the measured power density (Figure 6), stagnation was observed for reactors A2, B1, and B2, and a decrease for reactors A3, C1, C2, and C3. These changes can probably be attributed to the fact that the walls were no longer fed with greywater at this point.

To determine statistical differences for the power densities between the three walls in regard to the different reactor substrates the power densities of the walls, the values of reactors 1, 2, and 3 over the entire time shown in Figure 6 were used to derive a boxplot. for each wall (Figure 7).

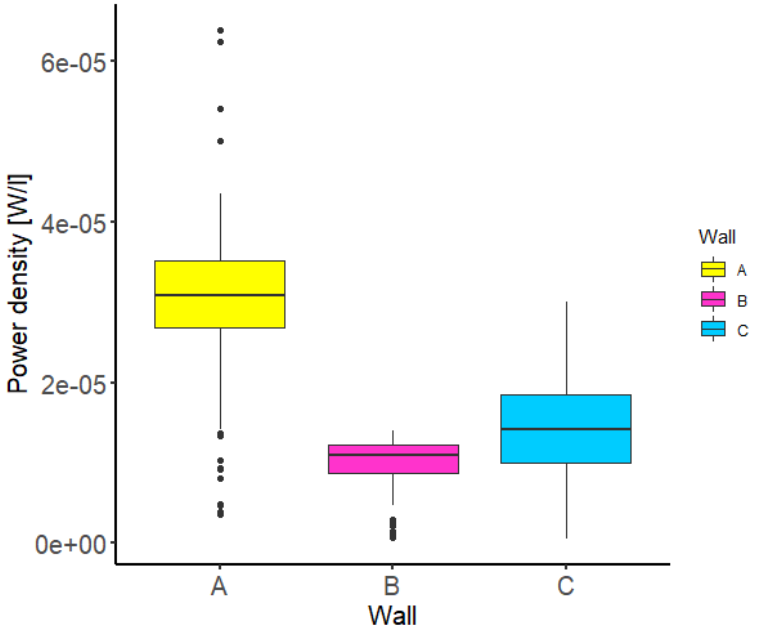

Figure 7: The calculated average power densities of the EGW-systems A (Vulkaponic substrate), B (Seramis expanded clay), and C (HDPE biocarriers), over the entire operation period of the system (starting with measuring campaign 1 and ending two months after measuring campaign 4).

To assess the power densities between the three walls with regard to the different reactor substrates (Figure 7), a one-way ANOVA was performed. It revealed that there was a statistically highly significant difference between the three reactor substrates ($F(2,240) = 121.2$, $p = < 0.001$). The results found after conducting Tukey's HSD Test for multiple comparisons are shown in Table 13.

Table 13: Results of the Tukey's HSD Test for multiple comparisons of the power densities in Walls A, B and C

		Walls	significance level	95% confidence interval
		A - B	p = < 0.001, (highly significant)	1.6E-05, 2.3E-05
		A - C	p = < 0.001, (highly significant)	1.2E-05, 1.9E-05
		B - C	p = < 0.01, (very significant)	-7.2E-06, -9.7E-07

According to Table 13, Wall A with Vulkaponic as reactor medium has a highly significant higher electrical power density than walls B and C. Wall B has a very significantly higher electrical power density than wall C. Therefore, it can be said that the reactor medium had an influence on the power generation.

To compare the changes in power density in the Walls A, B, and C, the values were sorted by measuring campaigns 1 to 4 (Figure 8).

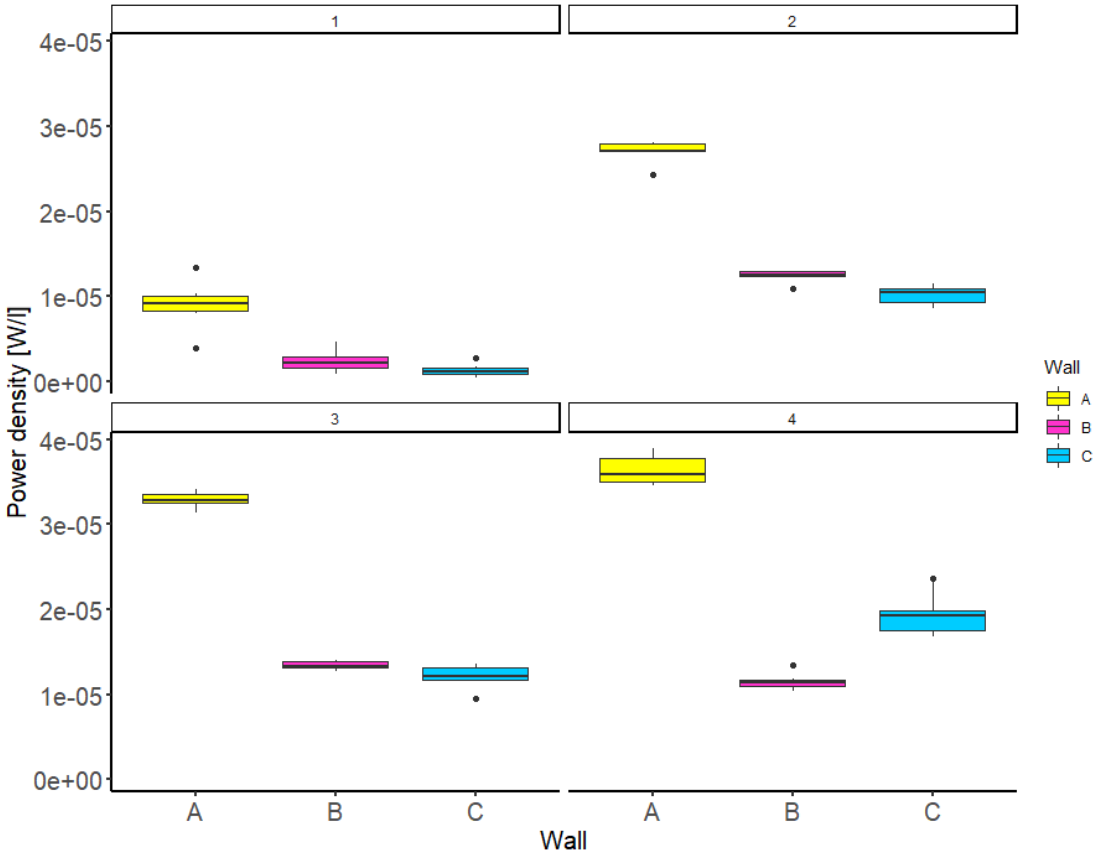

Figure 8: The calculated power densities of the EGW-systems A (Vulkaponic substrate), B (Seramis expanded clay), and C (HDPE biocarriers) sorted by measuring campaigns

As shown in Figure 6 and Figure 8 the power densities measured in walls A, B, and C increased with each measuring campaign.

4.3 Correlations of power density and water quality indicators

To discover possible correlations in the data of this study a Spearman's rank correlation matrix was created (Table 14).

Table 14: Spearman's rank correlation matrix comparing power density, the concentrations for TOC, COD, TN, and TP and DO. Stars indicate a statistical significance (* = p < 0.001 [highly significant] ** = p < 0.01 [very significant], * = p < 0.05 [significant])**

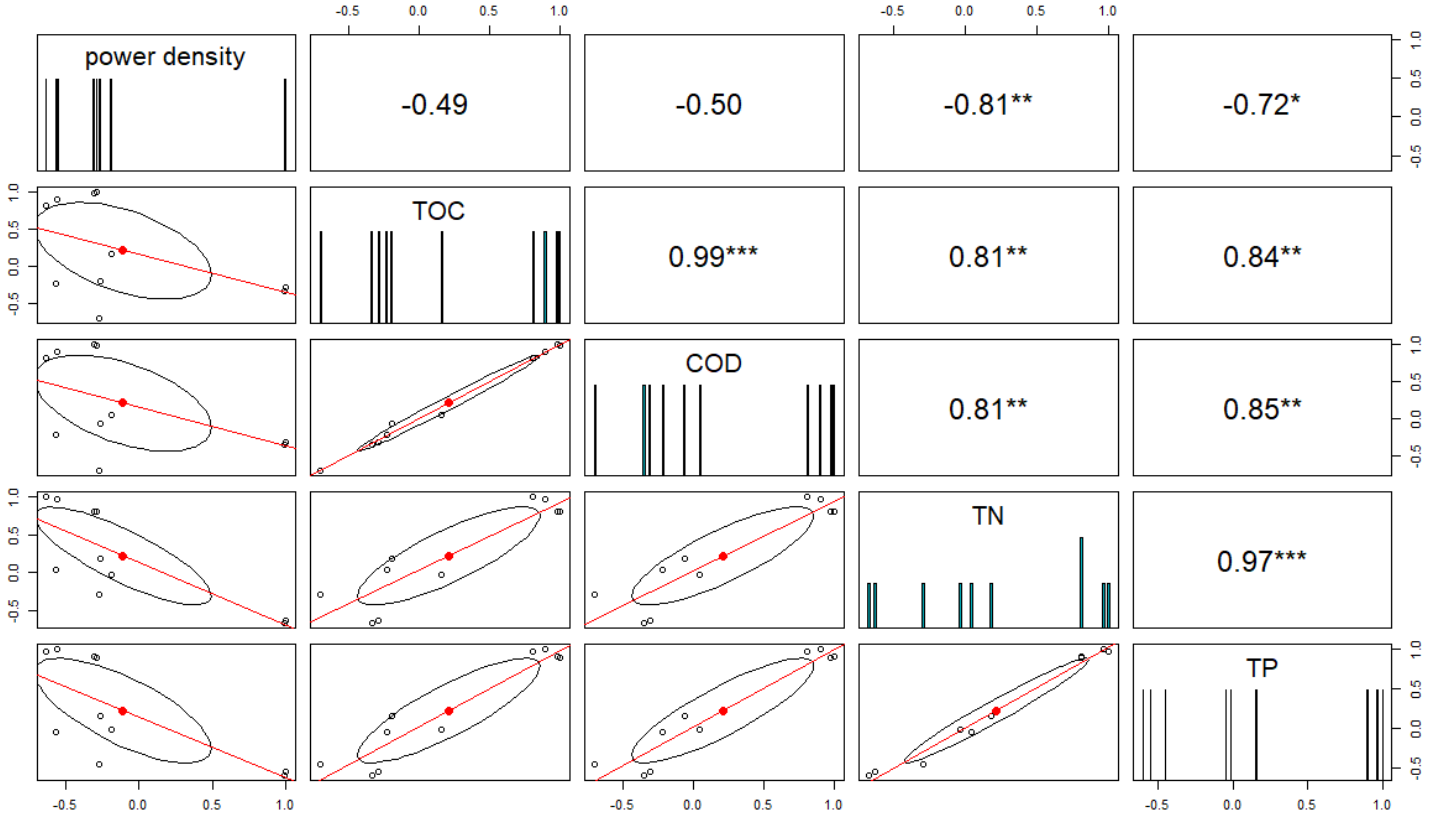

Strong positive correlations, that were very or highly significant were observed between all nutrient concentrations. These correlations were to be expected as there was a degradation of nutrients over time (Table 12).

Moderate negative, but non-significant correlations were witnessed between the power density and the TOC and COD concentrations.

A significant and a very significant, strong positive correlation was observed between the power density and TP and TN respectively.

Even though non-significant, the moderate negative correlation between the power density and TOC/COD, and the significant and a very significant, strong positive correlation between the power density and TP and TN respectively, could indicate that too high a wastewater load leads to a kind of "feeding shock", which reduces the product's electrical output.

The correlation between ORP and power density could not be included in the correlation matrix, because the data set of ORP was shorter. For that reason, a spearman’s ranked correlation test was conducted. It showed a non-significant ($p = 0.12$) moderately negative ($rho = -0.57$) correlation.

For the same reason, a spearman’s ranked correlation test between ORP and EC was conducted. It showed a significant ($p = 0.017$) negative ($rho = -0.78$) correlation.

5 Microbiology

5.1 Introduction

For an ECW or EGW to generate electric current, it is essential that a sufficiently large and stable population of exoelectrogenic bacteria colonize the anode. A number of exoelectrogenic bacteria are shown in Table 15.

Table 15: A selection of exoelectrogenic bacteria

Genus	Example of species	Metabolism	Literature sources
Rhodoferax	*R. ferrireducens*	Facultatively anaerobic	Chaudhuri and Lovley (2003)
Geobacter	*G. sulfurreducens*	Strictly anaerobic	Bond et al. (2002)
Aeromonas	*A. hydrophila*	Facultatively anaerobic	Pham et al. (2003)
Escherichia	*E. coli*	Facultatively aerobic	McKinlay and Zeikus (2004)
Shewanella	*S. putrefaciens*	Facultatively aerobic	Hernandez and Newman (2001); Kim et al. (2002)
Pseudomonas	*P. aeruginosa*	Strictly aerobic	Rabaey et al. (2005)

The currently best researched bacteria genera capable of exoelectrogenic reactions in MFC are *Shewanella* and *Geobacter* (Logan, 2008).

5.2 Materials and Methods

A metagenomic study of the bacterial population was performed with samples taken from the system used in Bezzola (2021). This system was also constructed from the NatureUp! (Gardena, Ulm, Germany) green wall system. The reactors were assembled in the same manner as in this study and also stacked into three walls (A, B and C).

The walls differed in water flows. Because all three reactors in wall A had identical water flows, the wall consisted of three reactors with a parallel flow. In the walls B and C, the three reactors each formed a single reactor with a serial flow (Figure 9).

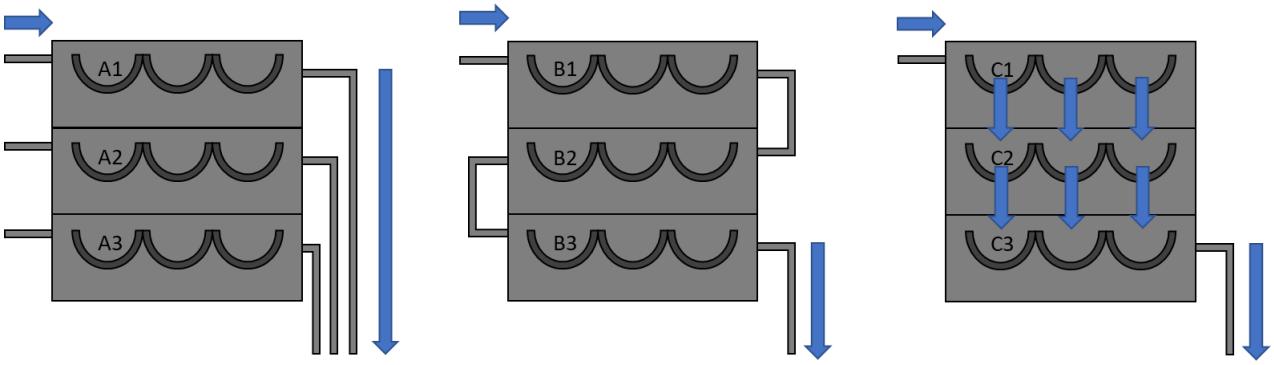

Figure 9: The water flow in walls A, B, and C in Bezzola (2021)

The electrodes in Bezzola (2021) were also constructed of biochar and SSM. The reactor medium in all three walls was Vulkaponic 3/8. Each system was fed with the same amount of greywater as the systems in this study during measuring campaigns 1-3 (Table 1).

From each of the reactors from the three walls A, B, and C, samples were taken from the reactor medium and from the biochar of the anode. All samples from the reactor medium and the biochar were mixed and subsequently subjected to a metagenomic analysis using 16S rRNA gene amplicon sequencing after DNA extraction. The analysis was done to determine the relative abundance of the top 20 genera in the biochar of the anode and the Vulkaponic in the reactor medium.

5.3 Results

The relative abundance of the top 20 genera found in the samples of Bezzola (2021) was visualized in a stacked barplot sorted by the walls A, B, and C.

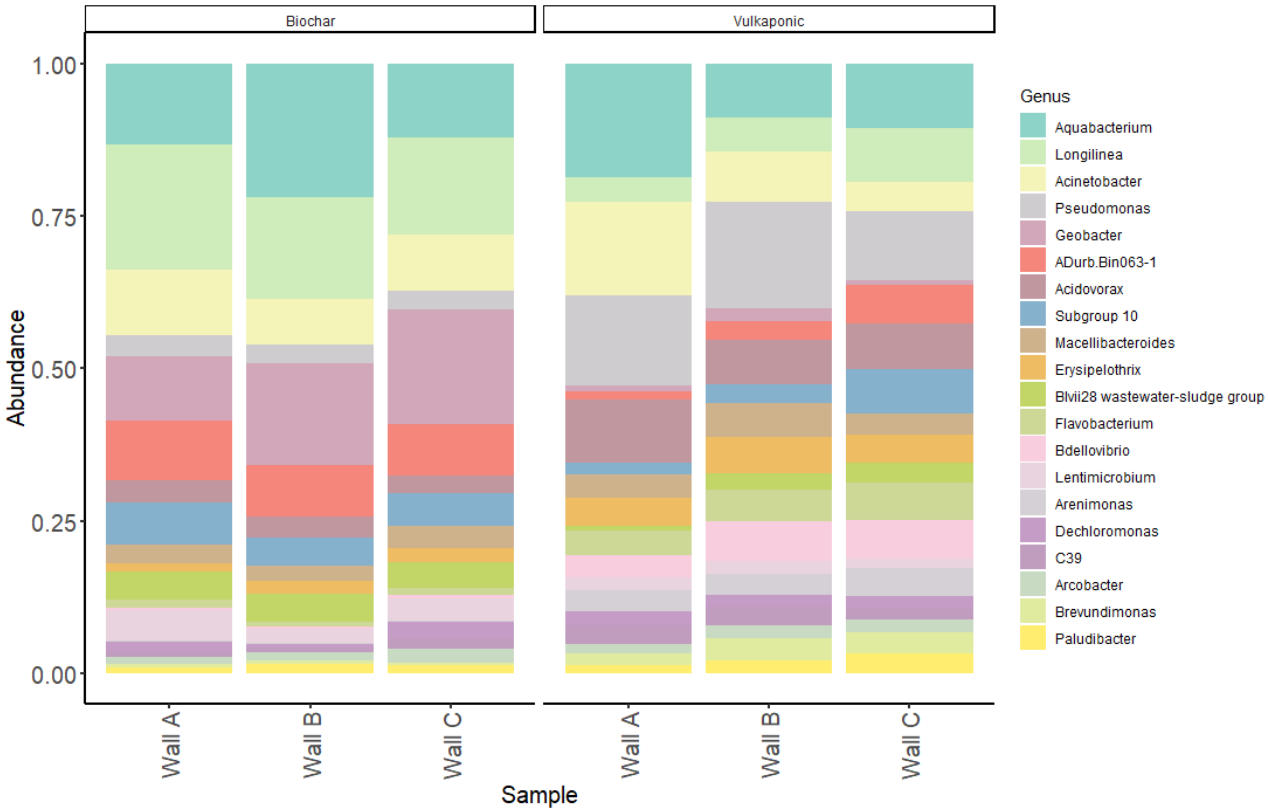

Figure 10: Relative abundance of the top 20 genera classified in the biochar layer of the electrodes and the Vulkaponic layer of the reactor media in EGWs (Bezzola, 2021)

The bacterial genera containing exoelectrogenic species shown in Figure 10 are *Geobacter* and *Pseudomonas*.

The considerable abundance of *Geobacter* in the biochar of the anode is consistent with the anaerobic conditions at the bottom of the reactors. However, their very marginal abundance in the reactor medium indicates prevalently aerobic conditions there.

The opposite effect to the genus *Geobacter* can be observed in the relative abundance of the genus *Pseudomonas*. This further indicates aerobic conditions in reactor medium.

In conclusion, a mixed population of exoelectrogenic bacteria may have formed in the reactors in Bezzola (2021) and thus probably also in this study.

6 Discussion

6.1 Possible usage of the generated power

The averaged maximum power per reactor was 5E-05 W/reactor. The peak maximum power density per reactor was four times higher at 20E-05 W/reactor. A Wall in this study covers an area of 0.363 m^2. The indoor green wall in the train station in Shin-Yamaguchi in Japan covers a surface of 400 m^2 (Blanc, 2013). It would be possible to fit approx. 1100 subunits, with an averaged maximum power of 5E-05 W per subunit or a peak maximum power density of 20E-05 W, on this area. This would result in a total power of 0.055 W and 0.22 W respectively. This is an extremely small power, which in reality could hardly operate an electrical consumer. For comparison, a modern LED light bulb requires about 6-9 W of power.

6.2 Comparison of the performance with literature

Table 16: Literature review electrochemical constructed wetlands sorted by reactor volume (smallest to largest). The power densities of literature review could not be directly compared, because some power densities were in W/m^2 and others in W/m^3. In order to obtain comparable data, the power was where possible calculated from the voltage and the external resistance for each source, according to Table 9. If possible, the maximum voltage or the averaged maximum voltage was used. To calculate the power density, the calculated power was divided by the respective reactor volume. The respective volume was calculated from the respective source or taken directly. If possible, the wetted volume was used.

Flow Type	Total Reactor Volume (l)	Voltage (mV)	External Resistance (Ohm)	Power (W)	Power density (W/l)	Max. COD removal (%)	max. HRT (h)	Anode material	Cathode material	Optimal distance Anode & Cathode (cm)	Substrate material	Used plants	Literature sources
vertical flow	**4.6**	**222.98**	**1000**	**5E-05**	**1.07E-05**	**63.7**	**48**	**biochar & SSM**	**biochar & SSM**	**10**	**Vulkaponic (3/8), Seramis & biocarriers**	**none**	**This study**
horizontal & vertical flow	**4.7**	**121.35**	**1000**	**1.47E-05**	**3.13E-06**	**85.9**	**120**	**biochar & SSM**	**biochar & SSM**	**9**	**Vulkaponic (3/8)**	**none**	**Bezzola, 2021**
Batch	0.5	400	1000	1.60E-04	3.20E-04	56	93.6	graphite or gravel	graphite felt	NA	graphite or gravel	none	Corbella et al., 2019
vertical flow	1.8	760			3.21E-04	95		granular graphite & graphite rods	platinum catalyst containing carbon cloth	7	gravel & glass wool	*Canna indica*	Srivastava et al., 2015
Batch	2.7	350	1000	1.23E-04	4.54E-05	86.7	48	C-fiber felt	C-fiber felt	30	quartz sand (2.8 mm)	*C. indica*	Wang et al., 2017

vertical subsurface flow	3.9	525.3	1000	2.76E-04	7.08E-05	95	72	granular activated carbon (GAC)	GAC, SSM or C-cloth	20	gravel (3-6 mm)	*Ipomoea aquatica*	Liu et al., 2014
Batch	5.4					75	96	NA	NA	32.5	Gravel (2-4 mm)	*C. indica*	Yadav et al., 2012
Batch	5.65	219	983	4.88E-05	8.64E-06	61.3	144	Graphite gravel (4-10 mm)	pyrrhotite	10	Dewatered alum sludge (DAS) (4-14 mm)	*Iris pseudacorus, Lythrum salicaria & Phragmites australis*	Yang et al., 2021
Upflow	11.3	560	1000	3.14E-04	2.77E-05		72	GAC (3-5 mm)	GAC & SSM	13.2	gravel	*I. aquatica*	Fang et al., 2017
Upflow	12.4	618	1000	3.82E-04	3.08E-05	85.65	72	GAC (3-5 mm)	GAC (3-5 mm) & SSM	20	gravel (3-6 mm)	*I. aquatica*	Fang et al., 2013
Upflow	17.3	265.8	1000	7.06E-05	4.08E-06	82.3	72	titanium mesh & activated carbon	titanium mesh	17.5	quartz sand & ceramsite (expanded clay)	*P. australis*	Xu et al., 2018
Upflow	19.1	421.7	1000	1.78E-04	9.32E-06	100	24	carbon felt	carbon felt	15	gravel (5.43 mm)	*Typha latifolia*	Oon et al., 2015
Upflow	30	639.8	12600	3.25E-05	1.08E-06	91.7	36	SSM & C-fiber-felt	SSM & C-fiber-felt	40	DAS (10 - 20 mm)	NA	Tang et al., 2019
Upflow	35.3		1000		6.19E-05	85.66	96	GAC & SSM	GAC & SSM	20	gravel	*I. aquatica*	Fang et al., 2015
HSSF	48	170	1000	2.89E-05	6.02E-07	61	62.4	graphite rods & SSM	graphite rods & SSM	10	gravel	*P. australis*	Corbella et al., 2016
horizontal subsurface flow (HSSF)	48.1	462	220	9.70E-04	2.02E-05	70	91.2	SSM	graphite felt	NA	gravel (4-8 mm)	none	Hartl et al., 2019
HSSF	108.1	120	120	1.20E-04	1.11E-06	95	76.8	graphite plate	graphite plate	25	gravel (9 mm) Ca-bentonite	*P. australis*	Villaseñor et al., 2013

Figure 11 shows that in this study the COD removal rate is around 20-30% lower than the majority of the comparative values. This is probably due to the fact that the HRT in this study was rather short with 48 hours compared to Bezzola (2021) with 120 hours. The question is, whether extending the HRT in this study from 48 to 120 hours would result in a comparable degradation rate to the comparable system used in Bezzola (2021). This assumption is supported by the fact, that the COD removal rates generally increase with increasing retention time. However, it has to be remembered that the shown in Figure 11 come from very different systems.

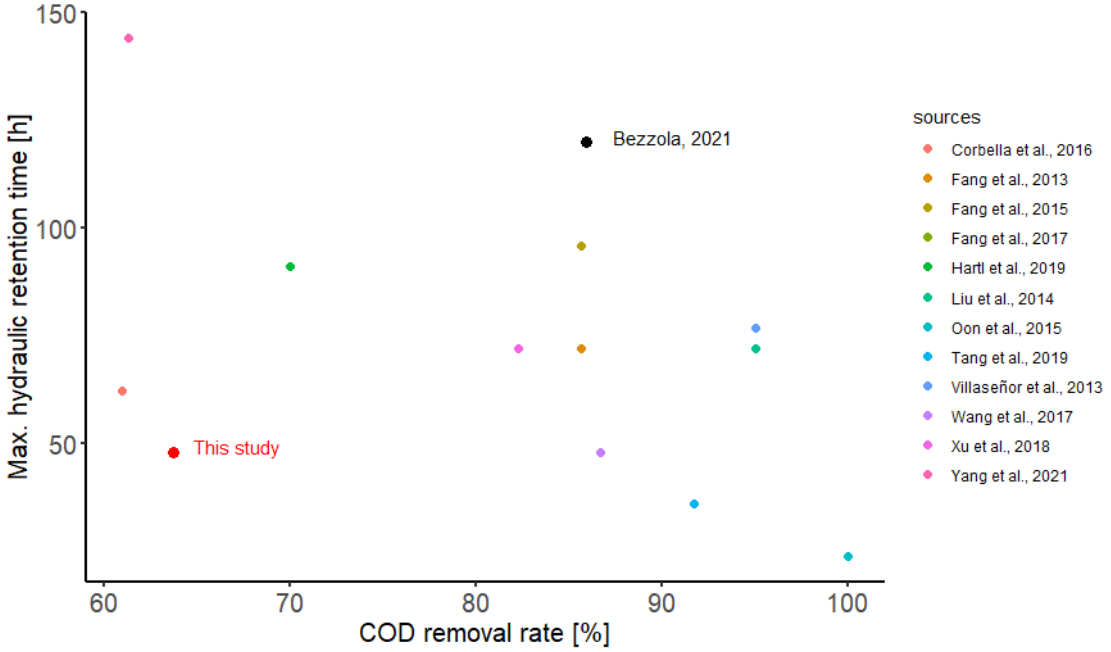

Figure 11: Plot comparing the HRT with the COD removal rate of the sources of the literature survey with the values from Bezzola (2021) and this study

Figure 12 shows a pronounced correlation between the power density and the COD removal rate. In this can also be seen, that overall power density in this study could be increased could be increased by a factor of about two, albeit at the cost of a lower COD removal rate, probably due to the shorter HRT.

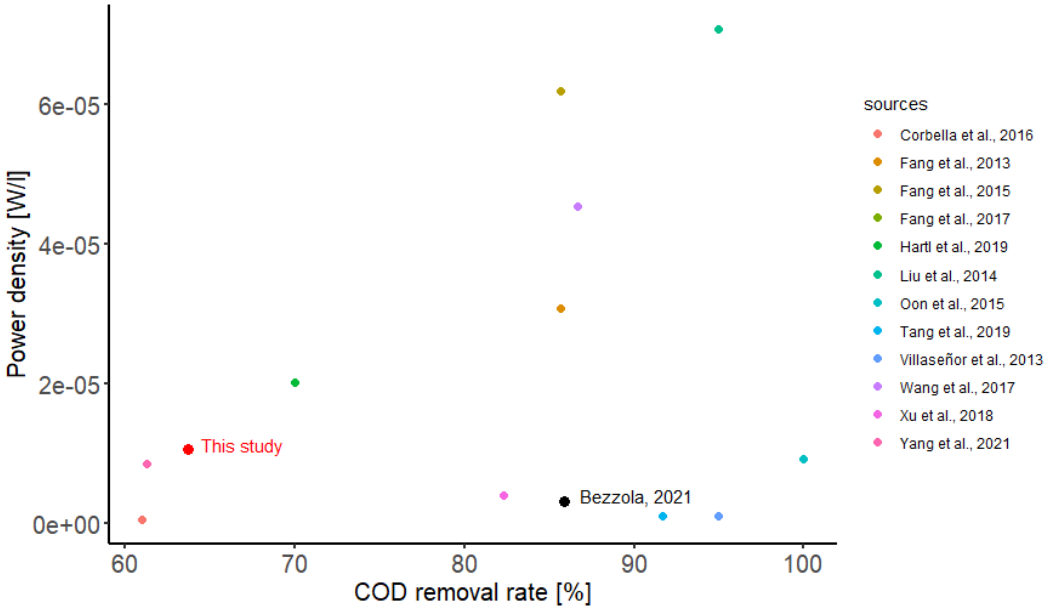

Figure 12: Plot comparing the power density with the COD removal rate of the sources of the literature survey with the values from Bezzola (2021) and this study. To improve the readability of the plot, the power density outliers of Corbella et al. (2016) and Srivastava et al. (2015) have been omitted.)

Even if there is a considerable scatter in the data, Figure 13 shows a correlation between the power density and the optimal distance between the anode and the cathode. The data of this study compares very well with the results of Bezzola (2021), as an increase of the optimal distance led to an increase of the power density of about 10%.

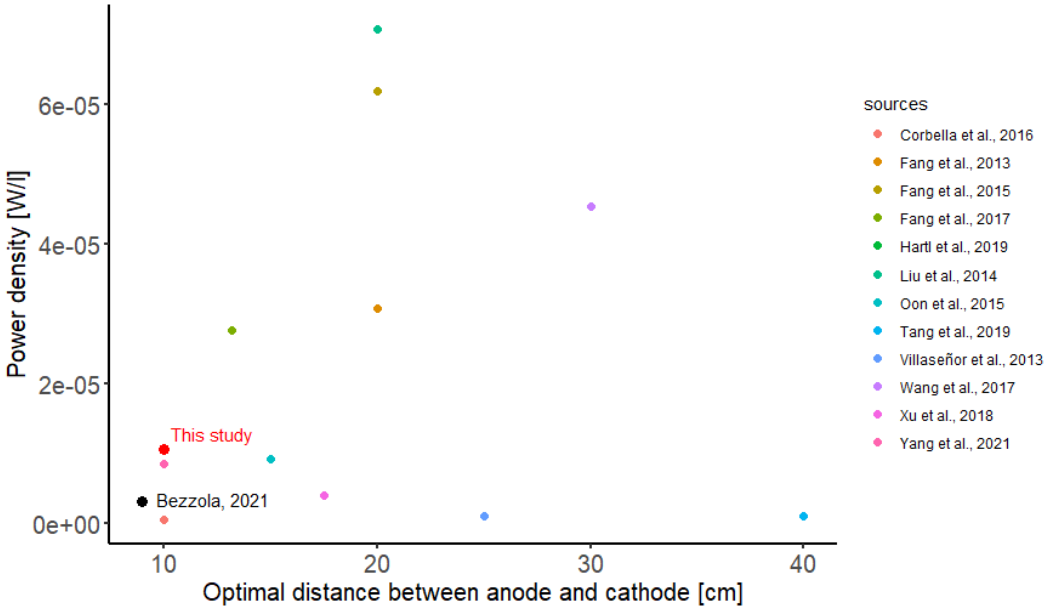

Figure 13: Plot comparing the power density with the optimal distance between anode and cathode of the sources of the literature survey with the values from Bezzola (2021) and this study. To improve the readability of the plot, the power density outliers of Corbella et al. (2016) and Srivastava et al. (2015) have been omitted.)

7 Conclusion

The modified wall design resulted in increased treatment performance compared to the system investigated in Bezzola (2021). However, it must be taken into account that the HRT in this study was comparatively shorter. By increasing the HRT, there is potential for a further improvement in treatment performance.

It was possible to increase the electrical power by increasing the electrode spacing by 10% (from 90 mm to 100 mm) by a factor of 2 on average, with significant differences within the walls (A, B, C).

In regard to the energy production, there are differences between the reactor media used. Vulkaponic generally results in the highest energy production values. This indicates that the substrate choice is another relevant parameter in green wall design.

However, the total power achieved is still very low. Given this, there is relatively little potential to produce energy economically even with a significantly enlarged plant of this design.

Although the power output is not sufficient to drive an electrical load, it could be used as an important indicator to characterize the state of the system in terms of bacterial activity. The generated electrical power could therefore be used in addition to the water quality parameters to optimally monitor, control and feed the system.

8 Bibliography

Asano, T., 2016. Artificial Recharge of Groundwater. Elsevier.

Bezzola, G.A., 2021. Construction and test of a fuel cell integrated into a green wall. Zürcher Hochschule für angewandte Wissenschaften (ZHAW), Wädenswil.

Blanc, P., 2013. Shin-Yamaguchi Station [WWW Document]. URL https://www.verticalgardenpatrickblanc.com/realisations/yamaguchi/shin-yamaguchi-station (accessed 7.4.21).

Bond, D.R., Holmes, D.E., Tender, L.M., Lovley, D.R., 2002. Electrode-Reducing Microorganisms That Harvest Energy from Marine Sediments. Science 295, 483–485. https://doi.org/10.1126/science.1066771

Bouwer, H., 2002. Artificial recharge of groundwater: hydrogeology and engineering. Hydrogeol. J. 10, 121–142. https://doi.org/10.1007/s10040-001-0182-4

Brix, H., 1994. Functions of Macrophytes in Constructed Wetlands. Water Sci. Technol. 29, 71–78. https://doi.org/10.2166/wst.1994.0160

Chaudhuri, S.K., Lovley, D.R., 2003. Electricity generation by direct oxidation of glucose in mediatorless microbial fuel cells. Nat. Biotechnol. 21, 1229–1232. https://doi.org/10.1038/nbt867

Corbella, C., Garfí, M., Puigagut, J., 2016. Long-term assessment of best cathode position to maximise microbial fuel cell performance in horizontal subsurface flow constructed wetlands. Sci. Total Environ. 563–564, 448–455. https://doi.org/10.1016/j.scitotenv.2016.03.170

Corbella, C., Garfí, M., Puigagut, J., 2014. Vertical redox profiles in treatment wetlands as function of hydraulic regime and macrophytes presence: Surveying the optimal scenario for microbial fuel cell implementation. Sci. Total Environ. 470–471, 754–758. https://doi.org/10.1016/j.scitotenv.2013.09.068

Corbella, C., Hartl, M., Fernandez-gatell, M., Puigagut, J., 2019. MFC-based biosensor for domestic wastewater COD assessment in constructed wetlands. Sci. Total Environ. 660, 218–226. https://doi.org/10.1016/j.scitotenv.2018.12.347

Davis, M.L., 2010. Water and Wastewater Engineering: Design Principles and Practice, First edition. ed. McGraw-Hill Education, New York.

De Gisi, S., Pica, R., Casella, P., Notarnicola, M., 2018. Dealing with a cluster of large centralized municipal wastewater treatment plants: A case study. Process Saf. Environ. Prot. 118, 268–278. https://doi.org/10.1016/j.psep.2018.07.002

Dotro, G., Langergraber, G., Molle, P., Nivala, J., Puigagut, J., Stein, O., von Sperling, M., 2017. Treatment Wetlands. IWA Publishing. https://doi.org/10.2166/9781780408774

Fan, Y., Wu, X., Shao, L., Han, M., Chen, B., Meng, J., Wang, P., Chen, G., 2021. Can constructed wetlands be more land efficient than centralized wastewater treatment systems? A case study based on direct and indirect land use. Sci. Total Environ. 770, 144841. https://doi.org/10.1016/j.scitotenv.2020.144841

Fang, Z., Cao, X., Li, Xuexiao, Wang, H., Li, Xianning, 2017. Electrode and azo dye decolorization performance in microbial-fuel-cell-coupled constructed wetlands with different electrode size during long-term wastewater treatment. Bioresour. Technol. 238, 450–460. https://doi.org/10.1016/j.biortech.2017.04.075

Fang, Z., Song, H., Cang, N., Li, X., 2015. Electricity production from Azo dye wastewater using a microbial fuel cell coupled constructed wetland operating under different operating conditions. Biosens. Bioelectron. 68, 135–141. https://doi.org/10.1016/j.bios.2014.12.047

Fang, Z., Song, H.-L., Cang, N., Li, X.-N., 2013. Performance of microbial fuel cell coupled constructed wetland system for decolorization of azo dye and bioelectricity generation. Bioresour. Technol. 144, 165–171. https://doi.org/10.1016/j.biortech.2013.06.073

Gross, A., Maimon, A., Alfiya, Y., Friedler, E., 2015. Greywater reuse. CRC Press, Boca Raton.

Hartl, M., Bedoya-Ríos, D.F., Fernández-Gatell, M., Rousseau, D.P.L., Du Laing, G., Garfí, M., Puigagut, J., 2019. Contaminants removal and bacterial activity enhancement along the flow path of constructed wetland microbial fuel cells. Sci. Total Environ. 652, 1195–1208. https://doi.org/10.1016/j.scitotenv.2018.10.234

Heinss, U., Morel, A., Moura, M., Schertenleib, R., 2004. Decentralized wastewater treatment - new concept and technologies for Vietnamese conditions 10.

Hernandez, M.E., Newman, D.K., 2001. Extracellular electron transfer. Cell. Mol. Life Sci. CMLS 58, 1562–1571. https://doi.org/10.1007/PL00000796

Hourlier, F., Masse, A., Jaouen, P., Lakel, A., Gerente, C., Faur, C., Le Cloirec, P., 2010. Formulation of synthetic greywater as an evaluation tool for wastewater recycling technologies. Environ. Technol. 31, 215–223. https://doi.org/10.1080/09593330903431547

Kim, H.J., Park, H.S., Hyun, M.S., Chang, I.S., Kim, M., Kim, B.H., 2002. A mediator-less microbial fuel cell using a metal reducing bacterium, Shewanella putrefaciens. Enzyme Microb. Technol. 30, 145–152. https://doi.org/10.1016/S0141-0229(01)00478-1

Laugesen, C.H., Fryd, O., Koottatep, T., Brix, H., 2010. Sustainable Wastewater Management in Developing Countries - New Paradigms and Case Studies from the Field. American Society of Civil Engineers (ASCE).

Liu, S., Song, H., Wei, S., Yang, F., Li, X., 2014. Bio-cathode materials evaluation and configuration optimization for power output of vertical subsurface flow constructed wetland — Microbial fuel cell systems. Bioresour. Technol. 166, 575–583. https://doi.org/10.1016/j.biortech.2014.05.104

Logan, B.E., 2008. Microbial Fuel Cells. John Wiley & Sons.

Mara, D., 2004. Domestic Wastewater Treatment in Developing Countries. Routledge, London. https://doi.org/10.4324/9781849771023

McKinlay, J.B., Zeikus, J.G., 2004. Extracellular Iron Reduction Is Mediated in Part by Neutral Red and Hydrogenase in Escherichia coli. Appl. Environ. Microbiol. 70, 3467–3474. https://doi.org/10.1128/AEM.70.6.3467-3474.2004

Miyazaki, S., Yamada, K., 2016. Shishi-Odoshi and Large Deviations. IEICE Proc. Ser. 48.

Novotny, V., Brown, P., 2007. Cities of the future. IWA Publishing.

Oon, Y.-L., Ong, S.-A., Ho, L.-N., Wong, Y.-S., Oon, Y.-S., Lehl, H.K., Thung, W.-E., 2015. Hybrid system up-flow constructed wetland integrated with microbial fuel cell for

simultaneous wastewater treatment and electricity generation. Bioresour. Technol. 186, 270–275. https://doi.org/10.1016/j.biortech.2015.03.014

Osorio de la Rosa, E., Vázquez Castillo, J., Carmona Campos, M., Barbosa Pool, G.R., Becerra Nuñez, G., Castillo Atoche, A., Ortegón Aguilar, J., 2019. Plant Microbial Fuel Cells–Based Energy Harvester System for Self-powered IoT Applications. Sensors 19, 1378. https://doi.org/10.3390/s19061378

Pham, C.A., Jung, S.J., Phung, N.T., Lee, J., Chang, I.S., Kim, B.H., Yi, H., Chun, J., 2003. A novel electrochemically active and Fe(III)-reducing bacterium phylogenetically related to Aeromonas hydrophila, isolated from a microbial fuel cell. FEMS Microbiol. Lett. 223, 129–134. https://doi.org/10.1016/S0378-1097(03)00354-9

Pop, M., 2019. Microbial Fuel Cells [WWW Document]. Lets Talk Sci. URL https://letstalkscience.ca/educational-resources/stem-in-context/microbial-fuel-cells (accessed 3.29.22).

Pradhan, S., Al-Ghamdi, S.G., Mackey, H.R., 2019. Greywater treatment by ornamental plants and media for an integrated green wall system. Int. Biodeterior. Biodegrad. 145, 104792. https://doi.org/10.1016/j.ibiod.2019.104792

Prodanovic, V., McCarthy, D., Hatt, B., Deletic, A., 2019. Designing green walls for greywater treatment: The role of plants and operational factors on nutrient removal. Ecol. Eng. 130, 184–195. https://doi.org/10.1016/j.ecoleng.2019.02.019

Rabaey, K., Boon, N., Höfte, M., Verstraete, W., 2005. Microbial Phenazine Production Enhances Electron Transfer in Biofuel Cells. Environ. Sci. Technol. 39, 3401–3408. https://doi.org/10.1021/es048563o

Rothausen, S.G.S.A., Conway, D., 2011. Greenhouse-gas emissions from energy use in the water sector. Nat. Clim. Change 1, 210–219. https://doi.org/10.1038/nclimate1147

Srivastava, P., Yadav, A.K., Mishra, B.K., 2015. The effects of microbial fuel cell integration into constructed wetland on the performance of constructed wetland. Bioresour. Technol., Microbial Fuel Cells 195, 223–230. https://doi.org/10.1016/j.biortech.2015.05.072

Tang, C., Zhao, Y., Kang, C., Yang, Y., Morgan, D., Xu, L., 2019. Towards concurrent pollutants removal and high energy harvesting in a pilot-scale CW-MFC: Insight into the cathode conditions and electrodes connection. Chem. Eng. J. 373, 150–160. https://doi.org/10.1016/j.cej.2019.05.035

Timmons, M.B., Ebeling, J.M., 2010. Recirculating aquaculture. Cayuga Aqua Ventures, Ithaca, NY.

U.N. General Assembly, 2017. Work of the Statistical Commission pertaining to the 2030 Agenda for Sustainable Development, U.N. GAOR.

UNESCO World Water Assessment Programme, 2017. The United Nations World Water Development Report, 2017. Wastewater: The Untapped Resource. UNESCO, Paris.

UN-Water, 2021. UN-Water, 2021: Summary Progress Update 2021 – SDG 6 – water and sanitation for all. Version: July 2021. Geneva, Switzerland.

Villaseñor, J., Capilla, P., Rodrigo, M.A., Cañizares, P., Fernández, F.J., 2013. Operation of a horizontal subsurface flow constructed wetland – Microbial fuel cell treating wastewater under different organic loading rates. Water Res. 47, 6731–6738. https://doi.org/10.1016/j.watres.2013.09.005

Wang, J., Song, X., Wang, Y., Bai, J., Bai, H., Yan, D., Cao, Y., Li, Y., Yu, Z., Dong, G., 2017. Bioelectricity generation, contaminant removal and bacterial community distribution as affected by substrate material size and aquatic macrophyte in constructed wetland-microbial fuel cell. Bioresour. Technol. 245, 372–378. https://doi.org/10.1016/j.biortech.2017.08.191

Xu, F., Cao, F., Kong, Q., Zhou, L., Yuan, Q., Zhu, Y., Wang, Q., Du, Y., Wang, Z., 2018. Electricity production and evolution of microbial community in the constructed wetland-microbial fuel cell. Chem. Eng. J. 339, 479–486. https://doi.org/10.1016/j.cej.2018.02.003

Yadav, A.K., Dash, P., Mohanty, A., Abbassi, R., Mishra, B.K., 2012. Performance assessment of innovative constructed wetland-microbial fuel cell for electricity production and dye removal. Ecol. Eng. 47, 126–131. https://doi.org/10.1016/j.ecoleng.2012.06.029

Yang, Y., Zhao, Y., Tang, C., Liu, R., Chen, T., 2021. Dual role of macrophytes in constructed wetland-microbial fuel cells using pyrrhotite as cathode material: A comparative assessment. Chemosphere 263, 128354. https://doi.org/10.1016/j.chemosphere.2020.128354

Appendix A: Correlation matrix of all compared parameters

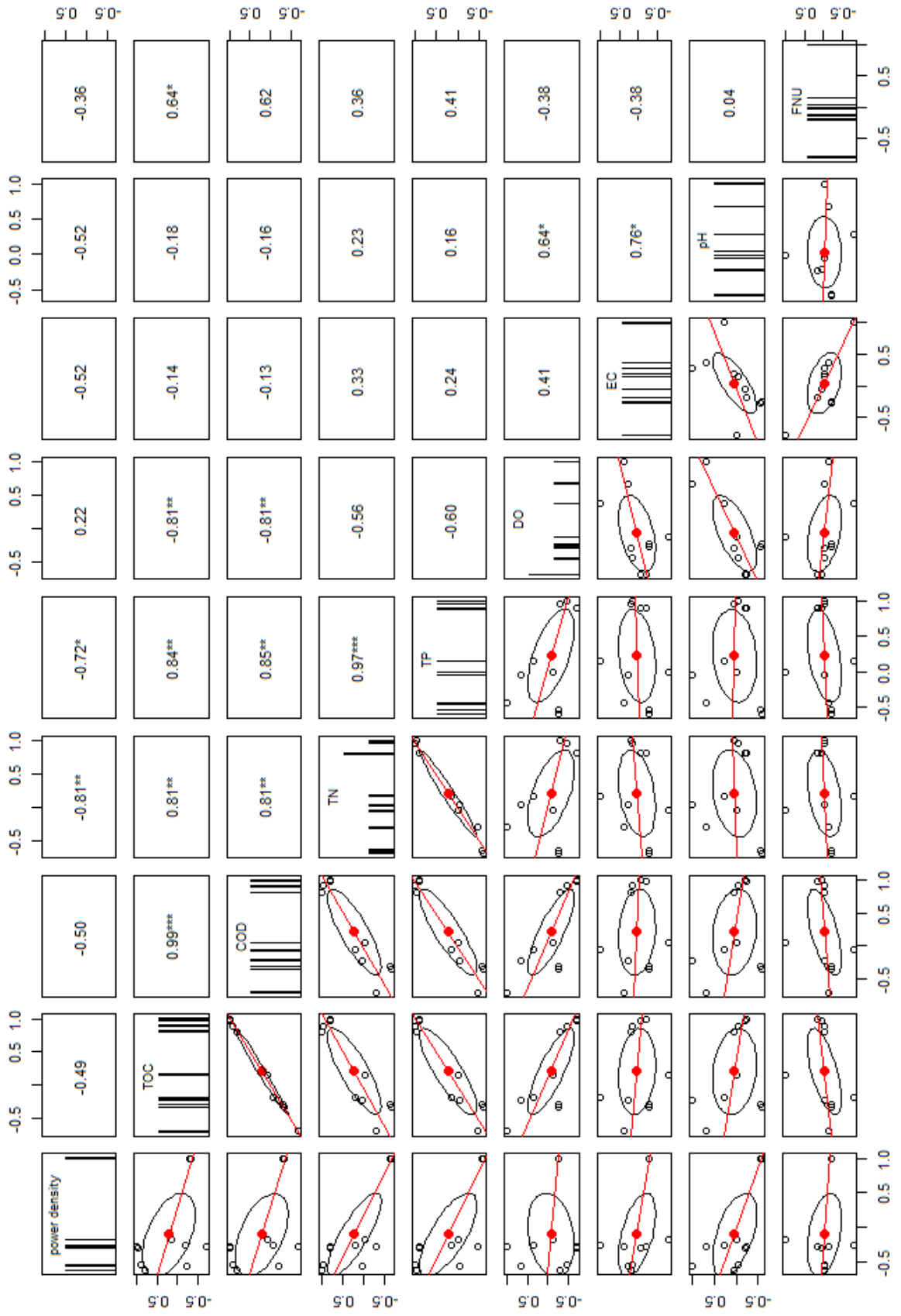

Appendix B: Images of the construction and operation of the system

Figure 14: Overview of the experimental installation with the three systems. From top to bottom: head tanks, inlet pipes with regulation valve (orange), mechanical dosing apparatus, and the three green walls. From left to right: Wall A (Vulkaponic substrate), Wall B (Seramis expanded clay), and Wall C (HDPE biocarriers). On the table in the foreground: data logger.

Figure 15: Wall A with Vulkaponic as reactor medium (reactors A1, A2, A3 from top to bottom)

Figure 16: Wall B with Seramis expanded clay as reactor medium (reactors B1, B2, B3 from top to bottom)

Figure 17: Wall C with HDPE biocarriers as reactor medium (reactors B1, B2, B3 from top to bottom)

Figure 18: Detailed view of a measuring tube (Reactor B1) to monitor abiotic parameters in the anaerobic zone

Figure 19: Detailed view of the mechanical dosing apparatus of Wall B, modeled after a Shishi-odoshi

Figure 20: Rear view of the plant with the collection tanks at the top and the return pipes to the reservoirs (blue barrels) at the bottom